Gradient-Free Measurements of Catalyst Plates Using a Berty Reactor

Lukas Thum*, Clara Marshall, Gudrun von der Waydbrink, Eugen Stotz, Katarzyna Skorupska and Robert Schlögl

DOI: 10.1002/cite.70001

Supporting Information available online

A Berty reactor modification is presented allowing kinetic investigations of catalyst plates or thin-film catalysts. Due to the narrow and defined spacing and high residence times, Da_{II} numbers below 0.001 can be achieved, excluding external mass transport. The reactor was tested in the methanol synthesis with wash-coated catalyst plates. Reaction parameters were varied over a large range proving the versatility of this system. The obtained activation energies for MeOH and CO formation are in good agreement with similar systems. At high pressures, the stirrer can homogenize the reaction mixture quite easily; above 500 rpm no effect of the stirrer on the performance can be observed. Even at ambient pressures, homogenization can be achieved, however, only at very high stirring speeds exceeding 4000 rpm.

Keywords: Berty reactor, Methanol synthesis, Reactor configuration, Reaction kinetics, Thin films

Received: February 16, 2025; *revised:* May 23, 2025; *accepted:* June 04, 2025

1 Introduction

Obtaining proper kinetic data is key to simulate and develop a process based on a catalyzed chemical reaction. Especially in heterogeneous catalysis, this sometimes can be quite challenging, needing to account for pressure drops along the catalyst bed, temperature profiles due to the heat of reaction, or external and internal mass transport. While the latter is a function of the catalyst morphology, trying to exclude the first three effects is most desirable for investigating catalysts and producing unperturbed kinetic data. Several different designs were proposed attempting to minimize these effects, resulting in an almost gradient-free reactor configuration. A prominent group of those are recirculation reactors. Whereas external recirculation devices are often challenging in their operation, especially in high-temperature applications with low vapor pressure components, internal recirculation reactors have been proven to be advantageous [1, 2]. While spinning basket reactors such as the Carberry reactor applies a high torque on the catalyst, making it a less desirable configuration for catalysts with low mechanical stability, the Berty reactor is more commonly used in a wide range of kinetic studies on powder catalysts [3–5] or monoliths [6] and also further improved allowing for applications at low pressures [7].

In this work, a commercial Berty reactor is adapted allowing for kinetic studies on film catalysts on flat substrates in the absence of external mass transport. The here chosen geometry of flat substrates aims to help building a bridge between studies based on a thin-film approach with performance catalytic materials employed in industry. The flat geometries are not limited to be exploited by alternative synthesis methods based on physical vapor deposition techniques applied in microelectronic, solar cell industry, or even catalytic model studies [8], it can also be used to study industrial performance catalysts under highly controlled conditions.

Manipulating the film properties of a catalytically active layer can have major effects on its performance. Finding

[1,2]Dr. Lukas Thum https://orcid.org/0000-0001-7622-2302 (lukas.thum@helmholtz-berlin.de), [1]Dr. Clara Marshall, [1,3]Gudrun von der Waydbrink, [1]Eugen Stotz, [1]Dr. Katarzyna Skorupska, [1,4]Prof. Dr. Robert Schlögl

[1]Fritz-Haber-Institute of the Max-Planck-Society, Department of Inorganic Chemistry, Zum Großen Windkanal 2–4, 12489 Berlin, Germany.

[2]Helmholtz-Zentrum Berlin für Materialien und Energie GmbH, PVcomB, Schwarzschildstr. 3, 12489 Berlin, Germany.

[3]Helmholtz-Zentrum Berlin für Materialien und Energie GmbH, Sample Environment Department, Albert-Einstein-Str. 15, 12489 Berlin, Germany.

[4]Max-Planck Institute for Chemical Energy Conversion, Department of Heterogeneous Reactions, Stiftstr. 34–36, 45470 Mülheim an der Ruhr, Germany.

the optimum thickness of a wash-coated layer is not only important to optimize the Thiele modulus [9] but can also affect the selectivity of the reaction [10]. Especially in tandem systems, tailoring the individual catalyst layers properly to achieve peak performance can be a demanding task and be simplified by employing stacked film structure instead of core-shell nanoparticles [11–13].

While this reactor concept cannot be scaled up, using microreactors for this purpose is often also challenging. Catalyst plates used in μ-reactors are often welded and therefore single-use. To optimize flow and mass transport in these systems, pre-existing knowledge of reaction parameters is needed for scaling in terms of, e.g., *Re*, Da_{II}, and heat transport [14]. A Bert-type reactor can be a reusable alternative for kinetic studies on such systems. To validate this concept, the reactor was tested in the methanol synthesis reaction from CO_2 using Kanthal plates wash-coated with a copper zinc alumina catalyst.

2 Experimental

2.1 Catalyst Synthesis

The copper-zinc-alumina catalyst was reproduced using a coprecipitation procedure reported before [15]. The metal solution was prepared by dissolving 164.29 g $Cu(NO_3)_2{\cdot}3H_2O$, 86.56 g $Zn(NO_3)_2{\cdot}6H_2O$, 11.22 g $Al(NO_3)_3{\cdot}9H_2O$, and 10 mL HNO_3 (65 %) in 1000 mL Millipore® water and the base solution by dissolving 171.32 g of anhydrous Na_2CO_3 in 1000 mL Millipore® water. The synthesis was performed in a semi-batch mode by adding 600.1 g of the metal solution to 400 mL water over a period of 30 min. The temperature was kept at 65 °C and the pH at 6.5 by dosing the base accordingly (in total 424.1 g). The obtained blue suspension was aged for 50 min at 65 °C, then filtered and washed four times with 1 L Millipore® water. The obtained solid was then suspended in 600 mL Millipore® water and spray-dried applying an inlet temperature of 180 °C, an outlet temperature of 80 °C, and a flow rate of 45 mL min^{-1}. A turquoise powder was received (internal ID S32774).

2.2 Catalyst Immobilization

The synthesized powder precursor was wash-coated on Kanthal® strips using an adapted procedure from the literature [16]. Kanthal® AF strips (1 mm thickness) were cut into pieces of around 15×10 mm^2, washed and cleaned thoroughly with water and isopropanol. Afterwards they were placed in a crucible and heated in a tube furnace applying a rate of 20 °C min^{-1} to a final temperature of 1100 °C in a constant flow of 80 mL min^{-1} oxygen and 320 mL min^{-1} argon (both from Air Liquide, 99.999 % purity). After 4 h at the final temperature, the furnace was cooled down also applying a rate of 20 °C min^{-1}. The appearance of the pieces changed to a matt grey (internal ID S36214).

A wash-coat mixture was prepared by dissolving 0.8 g polyvinyl alcohol (alquera; PVA) in 20 g water in a heated water bath. After complete dissolution of the PVA, 20 g glycerol (Fisher Scientific, reagent grade) was added to the mixture (internal ID S36211). An amount of 1.18 g of the washcoat mixture was mixed with 250 mg of the catalyst precursor material and stirred with a magnetic stirrer for two days. Nine of the oxidized Kanthal® pieces were placed on a plate and heated to 350 °C. The catalyst precursor washcoat mixture was filled in a commercial airbrush pistol equipped with a 200-µm nozzle supplied by 2 bar of argon. Using the airbrush, the whole catalyst precursor was slowly applied allowing the surface to dry and oxidize after each application. Once the whole solution was used up, the coated pieces were placed in a preheated muffle furnace at 300 °C for 2 h (internal ID S36215). Weighing of the plates before and after coating resulted in a mass gain of about 2 mg per 150 mm^2, which should result in layer thicknesses of around 10–30 µm assuming similar catalyst densities as comparable washcoats. Using such thin layers, internal mass transfer can be assumed to be negligible [17]. XRD pattern and SEM images of the samples can be found in Figs. S1–5 in the Supporting Information (SI).

2.3 Catalytic Tests

The setup for the catalytic testing is described in the next section. Six catalyst wafers were loaded in the sample holder pressurized with argon to 40 bar and heated to reaction temperature in a mixture of 33 % hydrogen and argon (both Westfalen AG, 99.999 % purity) under constant stirring at a speed of 3000 rpm. Upon reaching the reaction temperature, the feed is switched to 3:1:0.5 H_2:CO_2:Ar. Over the course of several days, the reaction parameters were varied to study the functionality of the reaction. The temperature was altered between 200 °C and 300 °C, the stirring speed between 0 and 5000 rpm, the pressure between 0 and 40 bar, and the total gas flow rate between 10 and 200 mL min^{-1}. The dataset and variations can be found in the supporting information Figs. S7–12. The conversion (X), selectivity (S), and yield (Y) were calculated by Eqs. (1), (2), and (3), respectively.

$$X = \frac{\sum n_{Products}}{\sum n_{Products} + \sum n_{Educts}} \tag{1}$$

$$S_i = \frac{n_i}{\sum n_{Products}} \tag{2}$$

$$Y_i = X \cdot S_i \tag{3}$$

As products, only carbon monoxide and methanol were considered. Methane was usually below the detection limit of the used GC and when detected in the ppm range, not affecting the calculation. The apparent activation energy was

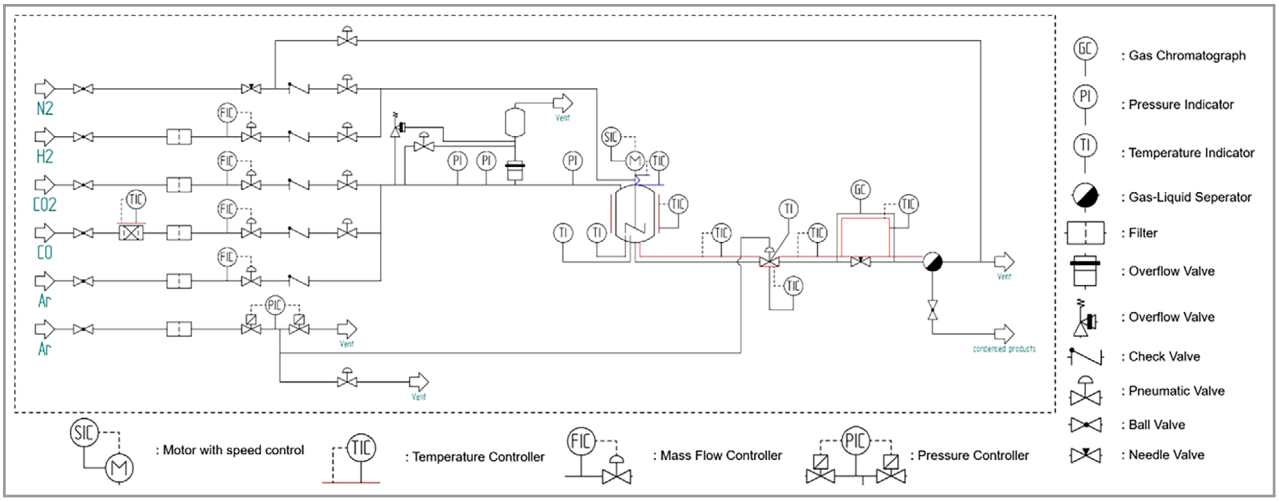

Figure 1. Flow chart of the here described Berty setup. The carbon monoxide line is equipped with a small heated fixed-bed reactor acting as a carbonyl trap. At the outlet an equilibar® is used to control the reactor pressure.

determined using the Arrhenius equation (Eq. (4)).

$$\ln(r_0) \sim -\frac{1}{T} \cdot \frac{E_a}{R} \tag{4}$$

Under the assumption and ignoring the thermal expansion of the gas can be neglected (Eqs. (5) and (6)), the equation simplifies to Eq. (7).

$$r = \frac{n_{in} - n_{out}}{\tau} \sim X, \; for small \; X \tag{5}$$

$$\tau = const. \tag{6}$$

$$\ln(X) \sim -\frac{1}{T} \cdot \frac{E_a}{R} \tag{7}$$

3 Setup

The here described setup was built around a commercial μ-Berty reactor supplied by Parker Autoclave Engineers; the flow chart is depicted in Fig. 1. For dosing the gases, mass flow controllers from the Bronkhorst® El-Flow® series are used for hydrogen, argon, and carbon monoxide; for carbon dioxide a Bronkhorst® MFC of the EL-Flow® Prestige series is applied, accounting for the changes of the thermodynamic properties of CO_2 at pressures close to its condensation pressure. The pressure control of the setup is realized by means of an equilibar® controlled by a Bronkhorst® pressure controller of the P-800 series. Using a steel membrane for the equilibar®, high temperatures can be applied in the downstream part of the reactor, avoiding condensation of the expected wet products streams from the CO_2 hydrogenation reaction. The feed consisting of hydrogen, carbon monoxide, carbon dioxide, and argon as an internal standard is split, using the hydrogen feed to purge the stirrer shaft, while the rest of the gases are fed over the common inlet. With hydrogen usually being the gas with the highest flow rate during hydrogenation reactions, as well the gas in the mixture with the lowest density, a de-mixing of the gases at high contact times in the stirrer shaft, or at worst, a condensation of reaction products can thus be efficiently prevented.

With the Berty reactor being a recycle reactor with high recycling rates [18], the here rather low applied flow rates and the two gas streams meeting above the stirrer, homogeneous mixing of the reactants in the reaction section is still expected. To avoid contamination by carbonyls in long-term experiments, a carbonyl trap is considered in the carbon monoxide line. All reaction products are kept in the gas phase to ensure an analysis of all the reaction products via online GC measurements. To prevent condensation, the downstream part of the setup in the high-pressure part can be heated up to 250 °C and the ambient pressure part up to 200 °C.

To account for an automated operation of the setup, several safety features are implemented. Normally open pneumatic valves in combination with restrictions allow a controlled pressure release in case of emergency, normally closed valves the immediate closing of the hazardous gases. Additionally, the setup is equipped with a purge line to efficiently remove toxic gases from the reactor. A gas warning system is coupled with the electronic controllers, automatically shutting the system off in case of strong leakages.

The autoclave and all its parts including the sample holder are made of Inconel® X-750. To facilitate the use of plate-like catalysts, the original sample holder of the Berty reactor (Fig. 2A) had to be re-created and adapted for the use with multiple plates (Figs. 2B–E). Using sink erosion, the challenging outer and inner structures could be manufactured with high precision, allowing a precise placement of the samples. For fixing the samples, recesses for exchangeable inserts were designed, allowing a defined distancing and adaption of the holder to work with changing sample sizes.

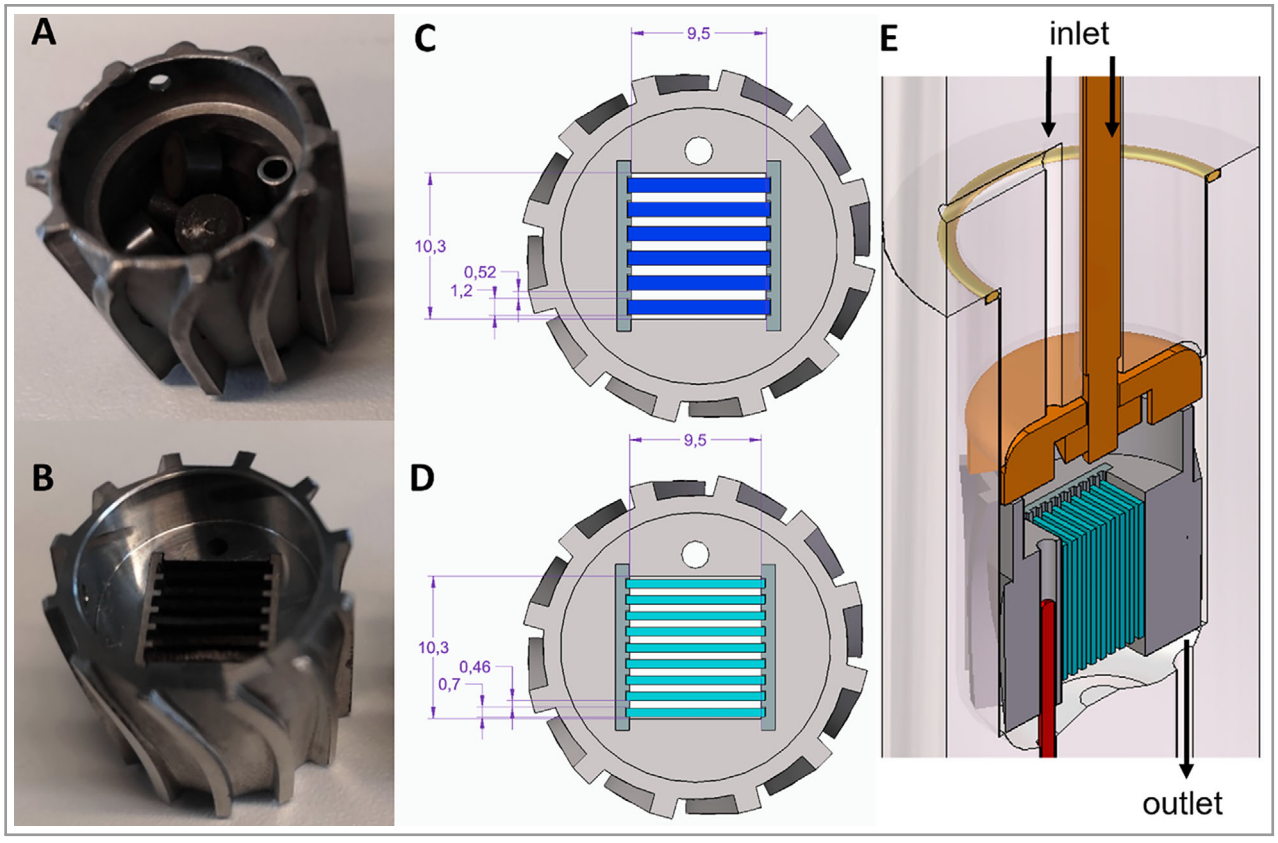

Figure 2. Photographs and schemes of the sample holders: the filled original sample holder (A), the filled adapted sample holder for plates (B) here, both shown without the fixing ring and mesh to secure the catalysts during operation, a scheme for the adapted holder with inserts for sample widths below 1200 µm (C), with inserts for samples widths below 700 µm (D), and the assembled reactor (E).

For initial tests, the gaps between the wafers were chosen to be directly relatable to the porosity of conventional catalyst beds [19]. With wafer sizes in the range of 600 µm to 1 mm, the filled sample holder has a porosity of 0.39–0.45, which is in the region of regular packed beds (Eqs. (8)–(10)).

$$\epsilon = 1 - \frac{V_{cat}}{V_{reactor}} \tag{8}$$

$$V_{reactor} = 10.3\ \text{mm} \cdot 9.5\ \text{mm} \cdot 15\ \text{mm} = 1468\ \text{mm}^3 \tag{9}$$

$$V_{cat} = [9 \times 0.6\ \text{mm}; 6 \times 1.0\ \text{mm}] \cdot 15\ \text{mm} \cdot 10\ \text{mm} = 810\text{–}900\ \text{mm}^3 \tag{10}$$

Using parallel wafers instead of packed beds, the formation of a laminar flow profile between the wafers cannot be excluded. In this case, to evaluate the possibility of diffusion limitations, without the application of elaborate DFT simulations, the Damköhler number of the second order can be determined. When the diffusion time of the gas in the channels t_D is significantly lower than the reaction time t_R, the influence of the diffusion on the measured reaction rate can be neglected (Eqs. (11) and (12)) [14].

$$Da_{II} = \frac{t_D}{t_R} \tag{11}$$

$$t_D = \frac{l^2}{2D} \tag{12}$$

The diffusion coefficient for gases under standard conditions can be generally approximated with 10^{-5} m^2s^{-1} [14]. Temperature and pressure dependence can be corrected using Eq. (13) [20].

$$D \sim \frac{T^{\frac{3}{2}}}{p} \tag{13}$$

Since in catalytic studies the reaction rates are often unknown and can change drastically with the investigated reaction, a general reaction time cannot be determined and has therefore to be evaluated individually for each case. However, in the here used setup, the range of possible residence times can be determined by the capacity of the installed mass flow controllers. Assuming a high internal circulation velocity induced by the stirrer, under optimal conditions the Berty reactor can be approximated with an ideal CSTR, meaning concentration gradients along the

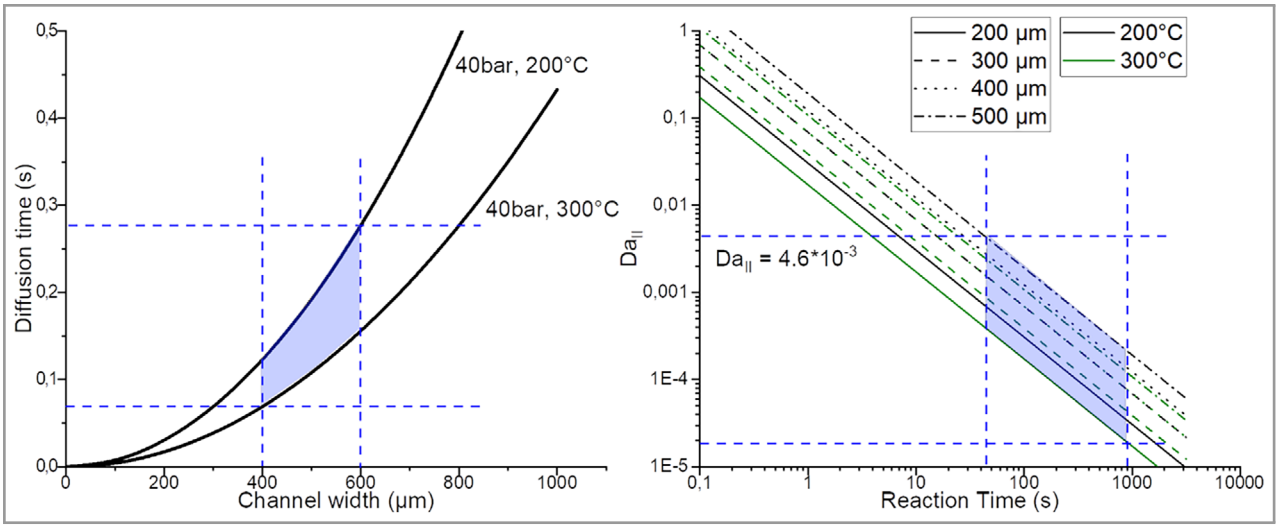

Figure 3. Estimation of the diffusion time as a function of the wafer distance (left); the blue area indicates the parameters fitting the configuration of the reactor used in this paper. Damköhler number of the second order at different reaction times (right), blue.

catalyst bed and the vessel below the stirrer are negligible. Therefore, as volume for calculating the residence time used for determining the Damköhler number, the whole circulated volume of the Berty autoclave can be considered.

An estimation of the Da_{II} of the here conducted methanol synthesis is illustrated in Fig. 3. The blue lines and areas mark the temperature range and flow range applied in this study. Since the nominal flow ranges of the mass flow controllers (MFCs) are fixed, reducing the working pressure results in a proportional shift of the reaction time. However, since the diffusion rate is also reciprocally related to the pressure, the diffusion time would shift in the same manner, resulting in identical Damköhler numbers. As expected from the narrow geometries with values for the Da_{II} of around 10^{-3}, external diffusion should play no role in this geometry.

4 Results and Discussion

As a proof-of-concept, the reactor setup was tested in the CO_2 hydrogenation reaction to methanol. Catalyst plates for the tests were obtained by spray-coating applying a $CuZnAlO_x$ precursor material on pre-oxidized Kanthal® plates and subsequent oxidation. XRD patterns of the oxidized coated plates show good agreement with the oxidized individual components (Fig. S1). After oxidation, the catalyst forms a porous film consisting of particle agglomerates with a homogeneous metal distribution (Figs. S2–5). SEM imaging after catalysis reveals the formation of fissures, indicating a limited stability of the produced washcoat, however, a sufficient stability was reached to verify the functionality of the setup, allowing time-on-stream experiments and several parameter variations over more than a ten days of experiments (Figs. S7 and S9). Kanthal® is an iron-chromium-aluminum alloy, which is often used as catalyst support in high-temperature applications, due to its high thermal stability and ability to form an inert, stable aluminum oxide layer on the surface via thermal treatment [21]. Its resistance and magnetic properties also such supports to be deployed in direct electrically heated applications, as, e.g., resistive heater, or as susceptor for induction heating; however, this is not in the scope of this work.

The key feature of the Berty reactor is the internal gas circulation induced by mechanical stirring. By changing the catalyst basket to an arrangement to vertically arranged plates, the pressure drop through the catalyst "bed" is significantly altered, which has a direct impact on the efficiency of stirring. Even though with the open rectangular slits resulting from the parallel arrangement of the samples the pressure drop will be significantly lower compared to a conventional packed bed (see Fig. S13 Ergun vs. Darcy-Weisbach equation in the SI), one must also consider the reduced overall cross section, resulting from changing the original round geometry to a rectangular one (compare Figs. 2A and 2B). The best way to verify the mixing behavior of the Berty reactor would be to observe the transient respond from a step-change in the gas concentration, which is, however, at low flow rates, low volumes, and elevated pressures not so easily performed [22].

Alternatively, the effect of the stirring rate on the measured kinetics of a chemical reaction can be investigated (Fig. 4). Without stirring on entering the reaction zone, the gas is expected to split according to the pressure drop ratio between the catalyst bed and the gap between reactor wall and sample holder and then exits the reactor through the bottom outlet. Only parts of the gas will be in contact with the catalyst and reactor to the products, therefore a low conversion and thus low production formation is expected. By stirring, the gas will experience an annular acceleration,

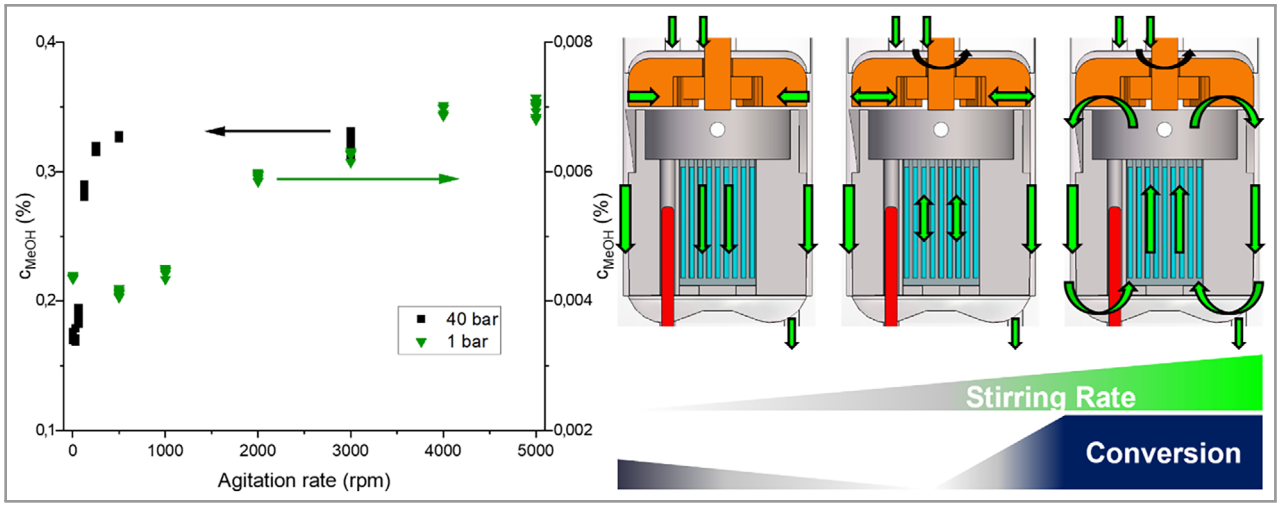

Figure 4. Impact of the stirring rate on the product formation at 180 mL min^{-1} gas feed, 6:2:1, H_2:CO_2:Ar, 240 °C applying different pressures (left). Schemes of the gas flow through the reactor at different stirring rates, with from left to right increasing stirring rates (right).

forcing it around the sample holder to the bottom of the autoclave. At the same time, the stirrer creates an upwards directed suction inducing an inverted flow from the bottom to the top of the catalyst bed. In case the induced momentum on the gas is very low, instead of improving the contact of the gas with the catalysts, even further decreasing the conversion of the chemical reaction, by preventing the gas to convectively enter the catalyst zone. Only when the stirrer represses a sufficient volume of gas, a high internal circulation can be reached and the fraction of gas bypassing the catalyst bed becomes negligible. In this case, a maximum yield is achieved and cannot be further improved by increasing the rotation rate of the stirrer (Fig. 4, right, Fig. S6 in the SI).

Fig. 4 (left) shows the methanol concentration versus the agitation rate during the methanol synthesis from CO_2 at 40 bar and ambient pressure. In the case of 40 bar, the impact of the stirrer levels out at rather low rotation rates. Already 500 rpm is sufficient to homogenize the reaction mixture, meaning the internal circulation rate far exceeds the external flow rate through the reactor. At low pressure, this looks quite different. The determined conversion hardly levels out at the maximum rotation rate of 5000 rpm, meaning that the bypassing gas cannot be ignored and the simplified assumption of a CSTR cannot be used. Applying the same standard flow rate at 40 bar compared to ambient pressure results in a factor 40 less velocity of the gas in the pressurized case, also requiring proportionally lower recycle rates to homogenize the system. Additionally, at higher pressures, the density of the reaction medium increases proportionally. Assuming, the stirrer, per rotation, always represses the same volume of a medium, at higher pressures, more mass is being moved, and the introduced momentum is proportionally increased. The impeller of the here used μ-Berty reactor from Autoclave Engineers has straight blades with a height of only 2.5 mm, explaining that only a small volume is moved per rotation, limiting this model to applications at elevated pressures [3]. For low-pressure application, the impeller speeds and shape have to be optimized to achieve the necessary high recycle rates [4, 22, 23].

For further validation of the usefulness of this design, a series of parameter variations were performed, varying temperature, pressure, and residence time, simulating diverse conditions applied in extensive kinetic investigations. The Berty reactor, in comparison to common plug-flow reactors, has the major advantage that the internal circulation rate by far exceeds the external feeding rate, allowing measurements over a broad range of residence times with negligible to no impact on the internal gas transport. Additionally, using high recirculation rates, a homogeneous catalyst temperature can, most of the time, be assumed. Provided that the catalyst is stable over the whole course of experimentation, the Berty reactor with only loading it once can provide data for full kinetic modeling. However, since this work aims to show the benefits of this Berty design for applications using catalyst films and the here used catalytic system is well known, profound kinetic modeling requiring a full experimental design is not performed in this study. In Fig. 5 the results of the parameter variation are presented; additional data of the performed experiments can be found in the SI.

With increasing temperature from 200 °C to 240 °C, more conversion is observed with both increasing the yield of CO from the reversed water-gas shift reaction (RWGS) as well as the methanol yield. With its stronger dependence on temperature, the activation energy for the CO formation was found to be significantly higher than the one for the methanol formation. The here determined values are in very

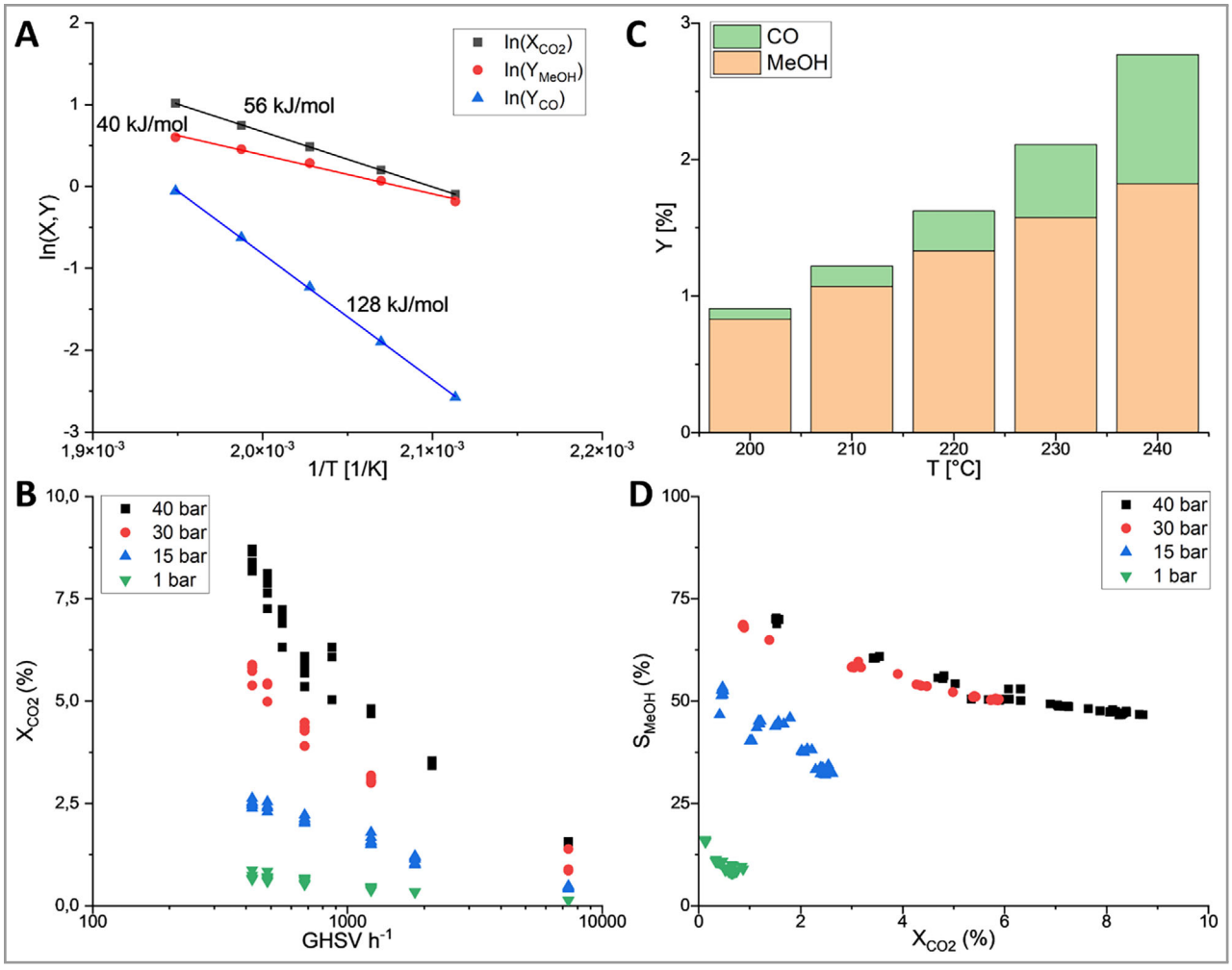

Figure 5. Arrhenius plots of the consumption of CO_2 and formation of the two products (top, left), and yields versus temperature (top, right). The experiments were conducted between 200 °C and 240 °C at 40 bar, applying a flow rate of 135 mL min^{-1} of 6:2:1 H_2:CO_2:Ar. Bottom graphs GHSV variation.

good agreement with those previously reported on a catalyst prepared in the same way before [15]. In Figs. 5B and 5D contact time variations are shown, producing clean *S*-*X* plots over a broad conversion range at different pressures with a single catalyst loading. The methanol-to-carbon monoxide ratio is best at pressures above 30 bar, while additional 10 bar pressure still increases the conversion; the selectivity does not change too much anymore, which is in line with other studies performed in Berty reactors [24]. Especially in the dataset collected at higher pressures, the data can get a little bit noisy.

There are several aspects to that, one being the MFCs. Working at a constant supply pressure of about 50 bar, the downstream pressure is varied between 1 and 40 bar. It was not possible to find suitable PID controlling parameters for this set of MFC working well in the whole range. A way to solve this could be the installation of a pressure stage directly behind the MFCs, allowing those to always work against a constant downstream pressure. A second problem is the vibration of the reactor itself. Though being mounted on vibration dampeners, parts of the vibration, especially along the steel lines, were still transferred to the MFCs, causing those sometimes to fluctuate. Further improvements can be done by installing more flexible gas lines to decouple the vibrations from the stirrer and the controllers. Over long-term experiments though, the Berty reactor performs very stable (Fig. S9 in the SI).

5 Conclusion

A catalytic test setup was designed around a μ-Berty reactor, allowing for kinetic characterization of catalyst plates. Its special geometry enables employment for studies on thin-film catalysts as well as performance materials in regard of optimizing washcoats in absence of external mass transport.

The reactor is a well-defined, re-usable alternative for often applied single-use plate reactors and microreactors, requiring pre-existing knowledge of the kinetic parameters for proper scaling. Though there is still room for improvement, CO_2 hydrogenation experiments under elevated pressure prove the applicability of this system for these kinds of studies.

The reactor performs well over a course of several days and allows the application of a broad range of reaction parameters with a single catalyst loading. Currently, this system does not operate well for applications close to ambient pressure. Nevertheless, the here developed sample holder can be easily adapted to fit other Berty reactors capable of operating under such conditions.

Supporting Information

Supporting information for this article can be found under DOI: https://doi.org/10.1002/cite.70001.

Acknowledgment

The authors acknowledge support from the Federal Ministry of Education and Research, Germany in the framework of the project CatLab (03EW0015A/B) and would like to thank Frank Girgsdies for XRD measurements and analysis as well as Zarah Gheisari for SEM imaging of the samples.

Open access funding enabled and organized by Projekt DEAL.

Symbols used

c_i	[mol L^{-1}]	concentration
D	[m^2s^{-1}]	diffusion coefficient
Da_{II}	[–]	second-order Damköhler number
E_a	[kJ mol^{-1}]	activation energy
GHSV	[h^{-1}]	gas hourly space velocity
l	[m]	lateral distance
n_i	[mol]	amount of material
p	[bar]	pressure
R	[J $K^{-1}mol^{-1}$]	gas constant (8.314)
r	[mol $L^{-1}s^{-1}$]	reaction rate
r_0	[mol $L^{-1}s^{-1}$]	initial reaction rate
Re	[–]	Reynolds number
S	[%]	selectivity
T	[K, °C]	temperature
t_D	[s]	diffusion time
TOS	[h]	time-on-stream
t_R	[s]	reaction time
V_i	[L]	volume
X	[%]	conversion
Y	[%]	yield

Greek letters

ϵ	[–]	porosity
T	[s]	residence time

Sub- and superscripts

i	reaction species
in	inlet
out	outlet

Abbreviations

cat	catalyst
CSTR	continuously stirred tank reactor
FIC	flow indicator controller
GC	gas chromatograph
MeOH	methanol
MFC	mass flow controller
PIC	pressure indicator controller
PVA	polyvinyl alcohol
SEM	scanning electron microscopy
TIC	temperature indicator controller
XRD	X-ray diffraction

References

[1] J. J. Carberry, Designing Laboratory Catalytic Reactors, *Ind. Eng. Chem.* **1964**, *56* (*11*), 39–46. DOI: https://doi.org/10.1021/ie50659a007

[2] J. M. Berty, Reactor for Vapor Phase Catalytic Studies, *Chem. Eng. Prog.* **1974**, *70* (5), 78–84.

[3] H. Hannoun, J. R. Regalbuto, Mixing Characteristics of a Micro-Berty Catalytic Reactor, *Ind. Eng. Chem. Res.* **1992**, *31* (*5*), 1288–1292. DOI: https://doi.org/10.1021/ie00005a008

[4] K. Ountaksinkul, S. Sripinun, P. Bumphenkiattikul, S. Bubphacharoen, A. Vongachariya, A. Jantharasuk, P. Praserthdam, S. Assabumrungrat, Characterization of Single-Phase Flow Hydrodynamics in a Berty Reactor Using Computational Fluid Dynamics (CFD), *React. Chem. Eng.* **2022**, *7* (*2*), 361–375. DOI: https://doi.org/10.1039/d1re00390a

[5] B. Kreitz, G. D. Wehinger, C. F. Goldsmith, T. Turek, Development of a Microkinetic Model for the CO_2 Methanation with an Automated Reaction Mechanism Generator, *Comput. Aided Chem Eng.* **2020**, *48*, 529–534. DOI: https://doi.org/10.1016/B978-0-12-823377-1.50089-6

[6] A. van de Riet, H. Vonk, X. Xiaoding, E. Otten, A. Cybulski, A. Stankiewicz, R. Edvinsson, J. A. Moulijn, Preparation, Characterization and Testing of Nickel on Alumina Monolithic Catalysts, *React. Kinet. Catal. Lett.* **1997**, *60* (*2*), 339–349. DOI: https://doi.org/10.1007/BF02475697

[7] Friedrich-Alexander-Universitaet Erlangen, Berty-Reaktor, DE 20 2014 006 675 U1, **2014**.

[8] M. S. Frei, F. L. P. Veenstra, D. Capeder, J. A. Stewart, D. Curulla-Ferré, A. J. Martín, C. Mondelli, J. Pérez-Ramírez, Microfabrication Enables Quantification of Interfacial Activity in Thermal Catalysis, *Small Methods* **2021**, *5* (*5*), 2001231. DOI: https://doi.org/10.1002/smtd.202001231

[9] M. J. Stutz, D. Poulikakos, Optimum Washcoat Thickness of a Monolith Reactor for Syngas Production by Partial Oxidation of Methane, *Chem. Eng. Sci.* **2008**, *63* (*7*), 1761–1770. DOI: https://doi.org/10.1016/j.ces.2007.11.032

[10] A. Aguirre, E. Scholman, J. van der Shaaf, M. F. Neira d'Angelo, Controlling the Selectivity in the Fischer-Tropsch Synthesis Using Foam Catalysts: An Integrated Experimental and Modeling Approach, *Chem. Eng. J.* **2021**, *409*, 128139. DOI: https://doi.org/10.1016/j.cej.2020.128139

[11] R. S. Ghosh, T. T. Le, T. Terlier, J. D. Rimer, M. P. Harold, D. Wang, Enhanced Selective Oxidation of Ammonia in a Pt/Al_2O_3@Cu/ZSM-5 Core-Shell Catalyst, *ACS Catal.* **2020**, *10* (*6*), 3604–3617. DOI: https://doi.org/10.1021/acscatal.9b04288

[12] Z. Wang, J. Qi, N. Yang, R. Yu, D. Wang, Core-Shell Nano/Microstructures for Heterogeneous Tandem Catalysis, *Mater. Chem. Front.* **2021**, *5* (*3*), 1126–1139. DOI: https://doi.org/10.1039/d0qm00538j

[13] G. Brösigke, J. U. Repke, R. Schomäcker, S. Matera, The Closer the Better? Theoretical Assessment of the Impact of Catalytic Site Separation for Bifunctional Core-Shell Catalyst Particles, *Chem. Eng. J.* **2022**, *446*, 1–31. DOI: https://doi.org/10.1016/j.cej.2022.136891

[14] D. Bošković, Reaktoren für spezielle technisch-chemische Prozesse: Mikrostrukturreaktoren, in *Handbuch ChemischeReaktoren* (Ed.: W. Reschetilowski), Springer, Berlin **2019**, 1211–1246. DOI: https://doi.org/10.1007/978-3-662-56444-8_44-1

[15] J. Schumann, T. Lunkenbein, A. Tarasov, N. Thomas, R. Schlögl, M. Behrens, Synthesis and Characterisation of a Highly Active Cu/ZnO:Al Catalyst, *ChemCatChem* **2014**, *6* (*10*), 2889–2897. DOI: https://doi.org/10.1002/cctc.201402278

[16] M. Ambrosetti, R. Balzarotti, C. Cristiani, G. Groppi, E. Tronconi, The Influence of the Washcoat Deposition Process on High Pore Density Open Cell Foams Activation for CO Catalytic Combustion, *Catalysts* **2018**, *8* (*11*), 510. DOI: https://doi.org/10.3390/catal8110510

[17] A. Montebelli, C. Giorgio, G. Groppi, E. Tronconi, S. Kohler, H. Johnsen, R. Myrstad, General Washcoating and Chemical Testing of a Commercial $Cu/ZnO/Al_2O_3$ Catalyst for the Methanol Synthesis over Copper Open-Cell Foams. *Appl. Catal., A* **2014**, *481*, 96–103. DOI: https://doi.org/10.1016/j.apcata.2014.05.005

[18] W. Reschetilowski, *Handbuch Chemische Reaktoren*, Springer, Berlin **2020**. DOI: https://doi.org/10.1007/978-3-662-56444-8

[19] M. Kraume, *Transportvorgänge in der Verfahrenstechnik*, Springer Vieweg, Berlin **2020**. DOI: https://doi.org/10.1007/978-3-662-60012-2

[20] *Mass Transfer in FluidSystems* (Eds.: D. R. Poirier, G. H. Geiger), Springer International Publishing, Cham **2016**, vol. *1999*. DOI: https://doi.org/10.1007/978-3-319-48090-9_14

[21] D. Zhang, L. Zhang, B. Liang, Y. Li, Effect of Acid Treatment on the High-Temperature Surface Oxidation Behavior of FeCrAlloy Foil Used for Methane Combustion Catalyst Support, *Ind. Eng. Chem. Res.* **2009**, *48* (*10*), 5117–5122. DOI: https://doi.org/10.1021/ie8019664

[22] S. D. Anderson, B. Kreitz, T. Turek, G. D. Wehinger, Assessment of Concentration and Temperature Distribution in a Berty Reactor for an Exothermic Reaction, *Ind. Eng. Chem. Res.* **2022**, *61* (*30*), 10790–10803. DOI: https://doi.org/10.1021/acs.iecr.2c01459

[23] K. Ountaksinkul, S. Wannakao, P. Praserthdam, S. Assabumrungrat, Intrinsic Kinetic Study of 1-Butene Isomerization over Magnesium Oxide Catalyst: Via a Berty Stationary Catalyst Basket Reactor, *RSC Adv.* **2020**, *10* (*60*), 36667–36677. DOI: https://doi.org/10.1039/d0ra05453d

[24] D. L. Chiavassa, J. Barrandeguy, A. L. Bonivardi, M. A. Baltanás, Methanol Synthesis from CO_2/H_2 Using Ga_2O_3-Pd/Silica Catalysts: Impact of Reaction Products, *Catal. Today* **2008**, *133–135* (*1–4*), 780–786. DOI: https://doi.org/10.1016/j.cattod.2007.11.034

